# Effects of Wind Flow and Topography on Snow Distribution and Liquid Water Content in Mountain Snowpack

Siobhan Ciafone

Department of Geography, University of Colorado Boulder

Defended April 5, 2021

Committee Members:

Noah Molotch, Geography (Thesis Advisor)

Keith Musselman, INSTAAR (Thesis Advisor)

Derek Brown, Atmospheric and Oceanic Sciences

Bill Travis, Geography, Honors Council Representative

TABLE OF CONTENTS

**Abstract**

Quantifying snowmelt behavior is valuable for understanding snow's implications for water availability, flood risk, and ecosystem health. Building off of ongoing analyses of observed lateral movement of liquid water through snow, this research used repeat ground penetrating radar (GPR) derived liquid water content (LWC) maps and terrestrial Light Detection and Ranging (LiDAR) derived snow depth maps to explore the effects of wind and topography on the distribution of liquid water within an alpine snowpack on Niwot Ridge, Colorado. Observations of wind speed and direction were combined with a simplified linear turbulence model to produce distributed estimates of wind speed for this alpine basin. In this paper, we assess how wind-driven snow accumulation and redistribution impact the subsequent patterns of liquid water in snow during the melt season. Using linear regression models relating topography and liquid water estimates, we explore the physical controls on snowmelt water availability. In areas of deep snow, wind flow patterns play a critical role in determining the storage and transmission of liquid water in the snowpack. The GPR and LiDAR data indicate that meltwater tends to collect at the interfaces of the snow layers, largely governed by wind dynamics, and this water moves rapidly along these interfaces to streams and rivers. We discuss how improved model representation of in-snow liquid water may be achieved through the aforementioned detailed measurements and analyses.

## Introduction

Snowmelt is a critical component of hydrology in mountainous regions. Quantifying snowmelt behavior accurately is necessary to properly understand and forecast water availability, flood risk, and ecosystem health and to predict the impact of climate change on water cycling. Winter snow melt is a significant source of water globally and one of the hydrologic processes most vulnerable to climate change (Musselman et al. 2017). Communities of semiarid climates downstream from snowy regions derive up to 80% of their water supply from snowmelt while changes to snow runoff processes due to climate warming will affect an estimated one-sixth of the global population (Barnett et al. 2005). Warming global temperatures are anticipated to cause a shift in precipitation phase from snow to rain, increased rain on flood events and subsequent increased flood risk, slower and earlier snowmelt rates, and decreased total snow accumulation and snowpack persistence (Musselman et al. 2018; Barnhart et al. 2016; Rauscher et al. 2008).

Earlier-than-average snowmelt timing is highly correlated with increased wildfire intensity and frequency (Westerling et al. 2006; Trujillo et al. 2012). According to a study by Westerling et al., in midlatitude regions, "56% of wildfires and 72% of area burned in wildfires occurred in early... snowmelt years" (Westerling et al. 2006). Earlier snowmelt is anticipated to cause decreased net carbon uptake by forests in seasonally snow-covered environments, potentially resulting in a 45% decrease in ablation-season carbon uptake by midcentury as meltwater availability will coincide with cooler temperatures and lower solar irradiance than historic growing seasons (Winchell et al. 2016).

Earlier snowmelt is anticipated to contribute to decreased streamflow as more melt water is lost to evaporation (Barnhart et al. 2016; Harpold et al. 2015). Meltwater can infiltrate through soil to reach subsurface flow only when soil field capacity is satisfied and soil is saturated

(Barnhart et al. 2016). Rapid snowmelt, especially when compounded with preferential flows paths that localize meltwater output, causes soil to reach saturation rapidly due to limited time for evapotranspiration to act on meltwater (Barnhart et al. 2016). Conversely, slower snow melt rates allow greater time for evapotranspiration to act on snowmelt and diminish the amount of meltwater that becomes subsurface flow (Barnhart et al. 2016, Harpold et al. 2015). Given the aforementioned impacts that decreased melt rates have on hydrologic partitioning, slower snowmelt rates are a significant threat to ecosystem health and water availability.

The timing and magnitude of meltwater has strong implications for the transmission of meltwater to soil moisture, streamflow, and groundwater recharge (Webb et al. 2020; Webb et al. 2018; Harpold et al. 2015). The springtime saturation of soil by meltwater controls the allocation of meltwater towards either groundwater recharge or streamflow or the loss of water through evapotranspiration (Webb et al. 2018 (a); Harpold et al. 2015). The seasonal saturation of the vadose zone, or the unsaturated zone situated between the saturated zone and the soil surface, controls stream connectivity and the release and distribution of nutrients from soil to streams and rivers, thus playing a consequential role in ecosystem nutrient cycling (Webb et al. 2018).

Typically, a snowpack must reach isothermal conditions, or 0° C across all depths, before meltwater is released (Kinar and Pomeroy 2015, DeWalle and Rango 2008). Ignoring impurities, an isothermal snowpack is composed of snow, water, and air (Kinar and Pomeroy 2015). Meltwater within a snowpack responds to gravity and flows vertically downward through snow to the snow-soil interface (SSI) unless diverted laterally by layers with less permeability such as ice lenses or wind crusts (DeWalle and Rango 2008, Webb et al. 2020). While the lateral movement of meltwater through snow is often ignored by hydrologic models (DeWalle and Rango 2008), the effect of permeability layers on meltwater flows is significant as these flowpaths have been shown to divert liquid water tens of meters prior to reaching the SSI (Eiriksson et al. 2013). Hydrologic models often oversimplify the movement of meltwater through a snowpack by only accounting for uniform, one-dimensional vertical percolation of meltwater through snow (Webb et al. 2020; Eiriksson et al. 2013). These models stand to improve estimates of runoff output by accounting for the spatio-temporal variability of meltwater movement within and across a snowpack, particularly at the basin-scale where cumulative lateral intra-snowpack flow may be significant (Webb et al. 2020).

While water flow within a snowpack is primarily governed by Darcy's law similarly to other porous media such as soil, saturated or near saturated zones on top of permeability layers divert water laterally (Eiriksson et al. 2013). These intra-snowpack flow paths atop permeability layers may converge downslope, resulting in localized meltwater output (Webb et al. 2020; Eiriksson et al. 2013). If infiltration rate exceeds the hydraulic conductivity of the soil, saturation will be reached and increased percolation of meltwater to groundwater or transmission to streamflow will occur (Webb et al. 2020; Winchell et al. 2016). Liquid water lateral intra-snowpack flow therefore can affect the quantity of meltwater that is allotted to soil moisture, groundwater recharge, and runoff (Webb et al. 2020). Spatio-temporal variability of runoff networks may impact timing of streamflow generation as well as water geochemistry, as the transmission and expulsion of meltwater through soil contributes to nutrient transportation (Webb et al. 2020).

The relative amount of meltwater transported through intra-snowpack flow paths increases with elevation, with intra-snowpack flow paths most influential in the alpine (Webb et al. 2020). Comparatively, snowpack at lower elevations can be more spatially discontinuous and interspersed with vegetation that can act as an efficient conduit to pass meltwater to soils. Alpine regions typically experience higher frequency snow events of greater magnitude. Increased frequency of snow events promotes the formation of snow layers, increasing snowpack stratification relative to lower elevation snowpacks (Webb et al. 2020). Enhanced stratification contributes to the potential formation of capillary barriers, or barriers to vertical meltwater infiltration through the snowpack (Webb et al. 2020). Meteorological conditions such as windflow and solar exposure generally increase with altitude as well and contribute to the formation of permeability barriers (Webb et al. 2020).

The higher frequency and magnitude of snow events in alpine regions contributes to greater total snow water equivalent (SWE) and greater cold content - the amount of energy required to raise the temperature of a snowpack such that temperatures equal an isothermal 0° C across all depths (DeWalle and Rango, 2008). Unsatisfied cold content may refreeze surface melt prior to the snowpack reaching isothermal conditions, promoting the formation of ice lenses (DeWalle and Rango 2008). Ice lenses are common layers of reduced meltwater permeability, formed by the refreezing of surface melt (Webb et al. 2020; Eiriksson et al. 2013).

As alpine environments lack tall vegetation, turbulent heat fluxes, radiation, and windflow instead exert the greatest control over snowpack depth variability and melt patterns (Webb et al. 2020; Musselman et al. 2015). The interaction of wind and topography may cause scouring and drifting, resulting in ecohydrological variations across basins during the melt season (Webb et al. 2020).

While vegetative control on snowpack beneath treeline may be significant due to sheltering and precipitation interception, snowpack in alpine environments where vegetation is scarce is more heavily impacted by wind patterns (Musselman et al. 2015). Wind and topography interactions in alpine environments contribute to the formation of persistent wind drifting, and sublimation may be more significantly impacted by wind flow patterns than by radiative flux (Musselman et al. 2015). While the effect of wind on snow accumulation affects sublimation rates as areas of deeper snow will melt more slowly, wind also affects sublimation rates as high wind flow increases heat and vapor flux on the snowpack surface (Musselman et al. 2015). Therefore, when attempting to quantify the variability of melt patterns over complex terrain in alpine environments, wind is an important factor to consider.

Historically, observing liquid water flow through snow has been limited due to challenges with observing snow while retaining its form (Webb et al. 2020; Webb et al. 2018 (b)). Until recently, observations of melt flow through snow have been two dimensional as they were only able to observe vertical movement of meltwater while non-destructive methods of observing snow were unable to identify meltwater flow paths (Webb et al. 2020). These complications compound upon the inherent difficulties of observing snow, as study areas with persistent snowpack are often difficult to access (López-Moreno et al. 2011). Recently, a new method of using terrestrial light detection and ranging (LiDAR) and ground penetrating radar (GPR) to map liquid water content in snow was developed (Webb et al. 2018 (b)), minimizing aspects of these challenges.

While remote sensing instrumentation and nivo-meteorological stations (e.g., Natural Resource Conservation Service SNOwpack TELemetry sites, SNOTEL) have advanced significantly in recent decades, the low spatial resolution of these measurements necessitates continued in situ data collection (López-Moreno et al. 2011, Deems et al. 2013). The inaccessibility and harsh conditions of study sites sought after for analysis of snow further complicates obtaining enough data for critical analysis (López-Moreno et al. 2011, Deems et al. 2013). These challenges necessitate that understanding of statistical relationships between snow characteristics such as volumetric LWC or snow depth and independent variables such as topography and wind speed be honed such that remotely sensed measurements may be accurately extrapolated to unsampled areas (López-Moreno et al. 2011). If the statistical relationship between topography, meteorology and snow variability is well understood, the need for extending the spatial and temporal coverage of in situ or remotely sensed measurements is minimized. Furthermore, understanding the nature of snow variability at the plot scale will deter the extrapolation of poorly representative measurements to the basin or regional scales (López-

Moreno et al. 2011). Understanding the impact of terrain and meteorology on snowpack variability such that representative sample sites may be selected is also of importance to snow energy balance modeling, which often relies on ground truth data to corroborate model outputs (López-Moreno et al. 2011).

This paper seeks to contribute to the body of knowledge surrounding the influence of wind velocity on snow accumulation and the effect of topographic variables, in this case aspect, slope angle, and elevation, on melt patterns in alpine snowpack by examining statistical relationships between these variables. Specifically, this paper seeks to understand the controls these variables exert on volumetric LWC in a melting snowpack. Through linear regression, the relationships of slope, aspect, elevation, and snow depth to volumetric LWC and the relationship of wind velocity to snow depth are explored using wind measurements, GIS analysis, and repeated surveys of Ground Penetrating Radar (GPR) and LiDAR scans. These relationships are evaluated over the course of one ablation season to determine the significance of these variables on volumetric LWC over time at the catchment scale.

Notably, wind velocity affects snow drifting primarily during the accumulation season while other relationships evaluated in this study are primarily ablation season processes. The relationship between snow depth and wind velocity will therefore be evaluated separately and will not be evaluated over the course of the melt season. Rather, the relationship between wind velocity and snow depth will be evaluated at all points simultaneously while other relationships will be evaluated by survey date.

I hypothesize the following:

1. Wind velocity and snow depth will have an inverse relationship as high winds transport snow while low winds deposit snow.
2. Slope angle will have an inverse relationship to LWC in snow because greater slope angle will encourage the downhill movement of liquid water. Conversely, low angle slopes will retain water due to lack of downhill liquid water flow and the deposition of liquid water from steeper slopes.
3. South facing slopes will exhibit greater LWC due to increased solar radiation on south facing slopes in the northern hemisphere.
4. As elevation does not vary significantly at the catchment scale, elevation will not significantly impact LWC in snow.

The relationship between snow depth and LWC is less easily predicted due to the potential variability of preferential flow paths across snow depths (an example of this is displayed in *Figure 1*). If preferential flow paths converge in areas of shallow snow depth such that the space between flow paths is condensed, volumetric LWC may be greater in shallow snowpack. As snow across a catchment may display continuous layering as all points are subject to the same meteorological events regardless of depth, areas of shallower snow may have condensed preferential flow paths when compared to deeper snow. Condensed flow paths would produce higher volumetric LWC values when compared with deeper snow with greater distance between permeability layers and subsequent flow paths. Alternatively, snow layering and subsequent preferential flow paths may vary across the catchment. Areas of deeper snow may have more preferential flow paths than shallower snow. If this is the case, the greater quantity of preferential flow paths present in deeper snow would contribute to greater volumetric LWC in areas of deeper snow.

Additionally, the greater cold content of deeper snow would contribute to an inverse relationship between snow depth and LWC, as more heating would have to occur before the snowpack reached isothermal conditions. A shallower snowpack may reach isothermal conditions and begin melting more quickly than deeper snow.

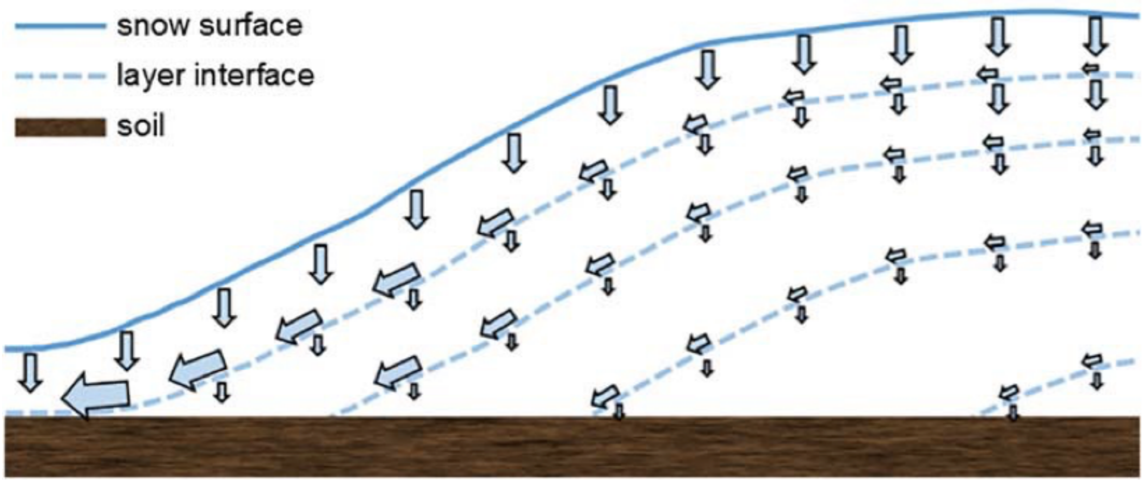


*Figure 1.* Liquid water moves laterally through a snowpack across layer interfaces before reaching the snow-soil interface. (Ryan et al. 2018.) In this image, areas of deeper snow have more permeability layers, labeled as 'layer interface', while shallower snow has fewer permeability layers. This image suggests that areas of deeper snow may have higher LWC due to greater permeability layers.

## Methods

*Study Area*

This study was conducted at the 0.3 $km^2$ alpine headwater catchment (Saddle), part of the Niwot Ridge Long Term Ecological Research site (LTER) in northern Colorado *(Figure 1)*. The Saddle sits in the Indian Peaks wilderness of the Colorado Rockies and is roughly a half mile east of the Continental Divide. 80% of the Saddle is above tree line and elevation ranges from 3,400- 3650 m a.s.l. The Saddle Catchment contributes to Green Lakes Valley, the headwaters of the Boulder Creek Watershed. Long term meteorological stations on the saddle provide ten minute wind speed and direction data, used with elevation data to map wind distribution in this study. The study area is in the traditional territory of Cheyenne, Arapahoe, and Ute nations.

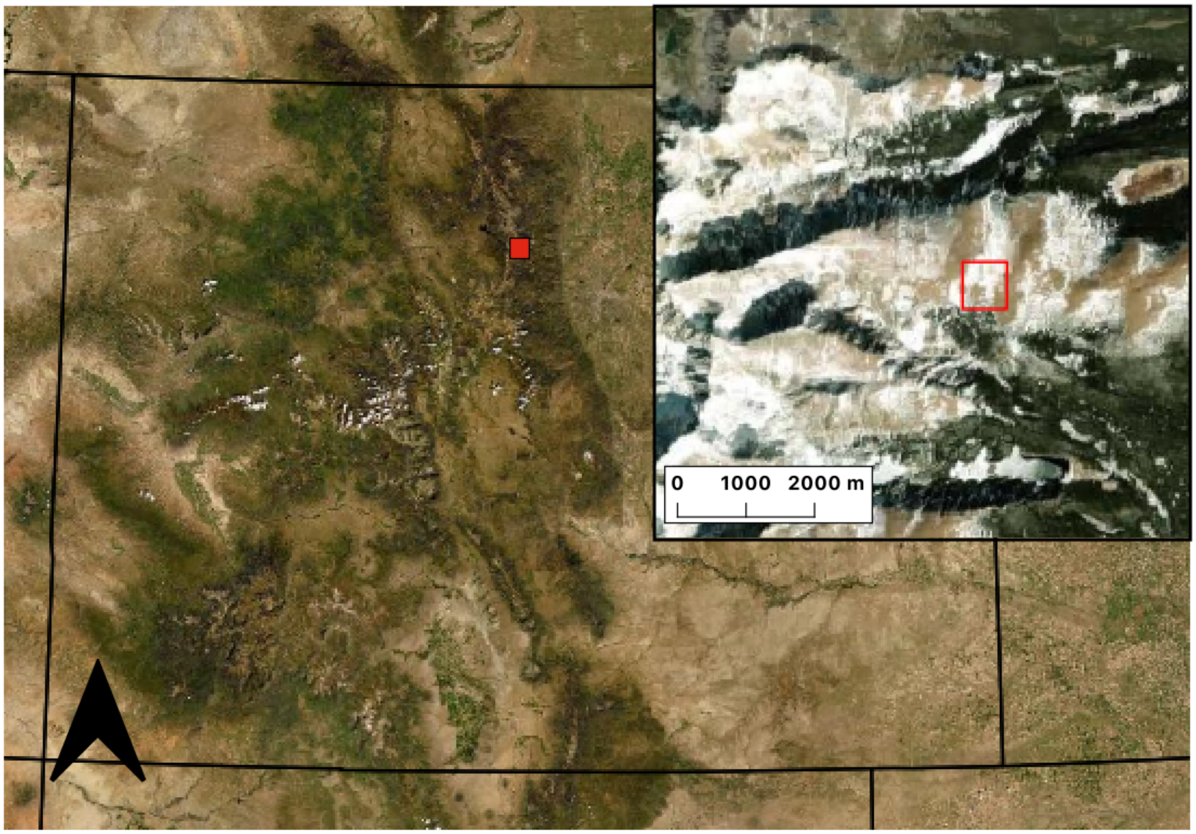


*Figure 1.* The location of the study site in Northern Colorado. Inset is a closer view of the study site, indicated by a red box.

Slope angles at the Saddle range from less than 1° to nearly 28° and aspects are primarily south, southeast, and east facing (*Figure 2*). As the Saddle is primarily above treeline, interception of snowfall by vegetation is negligible. Winds blow strongly and frequently. The variable topography and high winds of the Saddle cause scouring and drifting. High winds and variable snow depth and topography make this location highly suitable for this study.

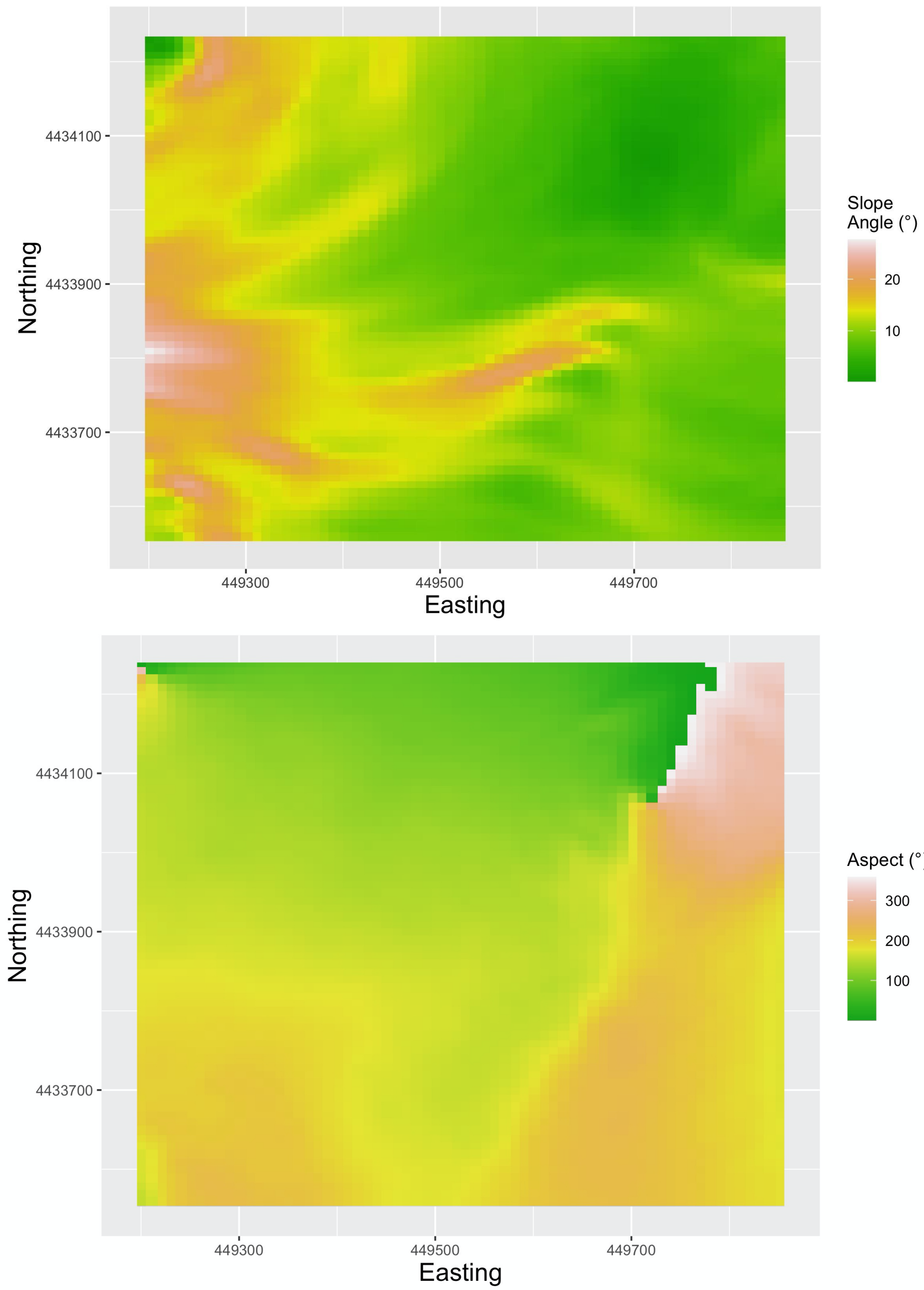


*Figure 2.* Slope angle (A) and aspect (B) of the study area. Aspect category is determined by degree angle, with greater than 337.5-360.0° and 0-22.5° categorized as north facing, angles greater than 22.5° and less than or equal to 67.5° categorized as northeast facing, angles greater than 67.5° or less than or equal to 112.5° categorized as east facing, angles greater than 112.5° and less than or equal to 157.5° categorized as southeast facing, angles greater than 157.5° and less than and less than or equal to 202.5° categorized as south facing, angles greater than 202.5° and less than or equal to 247.5° categorized as southwest facing, angles greater than 247.5° and less than or equal to 292.5° categorized as west facing, and angles greater than 292.5° and less than or equal to 337.5 categorized as northeast facing.

*Wind Rose and Wind flow Modeling*

To summarize wind velocity across the Saddle, 10-minute raw wind speed and direction data from a meteorological station on the Saddle was averaged hourly over the 2019 water year (Morse, J., M. Losleben, and Niwot Ridge LTER. 2020) and displayed in a wind rose (*Figure 3*). In order to average 10-minute data, vector mean wind direction was averaged through the following calculations:

$$V_{east}\,[i] \;=\; mean(WS[i] * sin\,(WD[i] * \frac{\pi}{180}))$$

$$V_{north}\,[i] \;=\; mean(WS[i] * cosine\,(WD[i] * \frac{\pi}{180}))$$

$$mean_{WD} \;=\; arctan2(V_{east}, V_{north})) * \frac{180}{\pi}$$

$$mean_{WD} \;=\; (180 + mean_{WD})$$

$$mean_{WS} \;=\; \sqrt{(V_{east}{}^{2} + V_{north}{}^{2})}$$

Where $V_{east}$ is an easterly vector, $V_{north}$ is a northerly vector, $[i]$ is any timestamp, *WS* is wind speed, and *WD* is wind direction.

Averaged wind speed and direction data indicated that 41.71% of wind originated from the southwest, 26.52% originated from the west, 12.43% originated from the South, 7.26% originated from the northwest, 5.57% originated from the southeast, 3.4% originated from the north, 1.71% originated from the northeast, and 1.41% originated from the east (*Figure 3,* **table 1**).

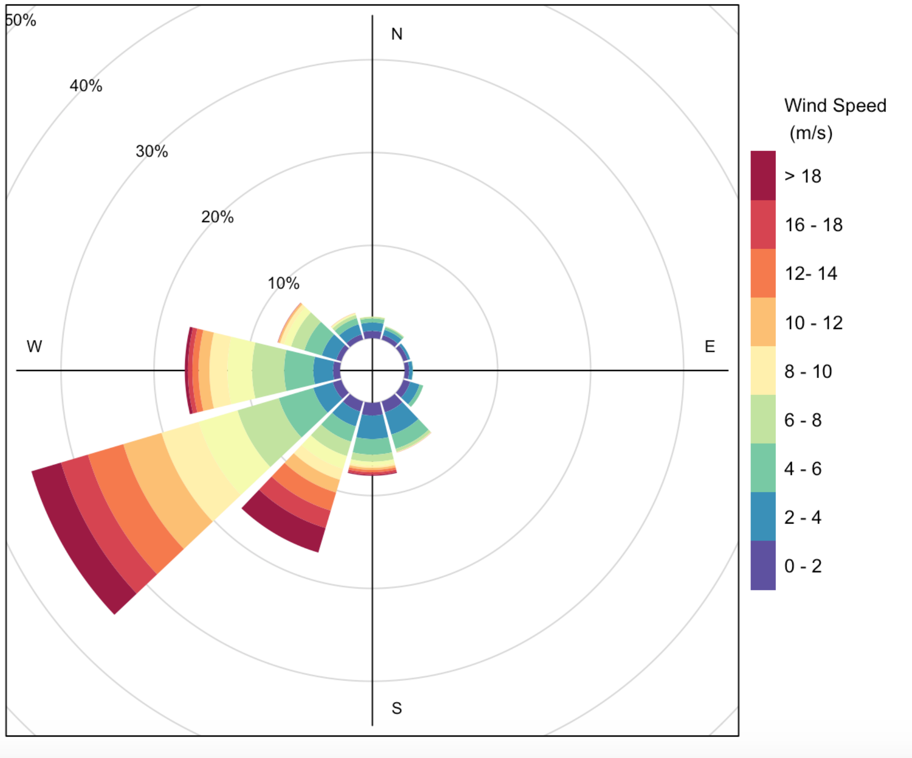


*Figure 3.* Wind direction and velocity of the Saddle Catchment averaged over the 2019 water year. This graphic illustrates that wind over the Saddle primarily originates from the Southwest, West, and South.

**Table 1.** Averaged hourly wind velocity and direction data for the 2019 water year. Data was used to populate the wind rose (*Figure 1*).

| | **E** | **N** | **NE** | **NW** | **S** | **SE** | **SW** | **W** | **Grand Total** |
|---|---|---|---|---|---|---|---|---|---|
| **1-4** | 0.01 | 0.02 | 0.01 | 0.03 | 0.06 | 0.04 | 0.05 | 0.04 | 0.27 |
| **4-8** | 0.00 | 0.01 | 0.00 | 0.03 | 0.04 | 0.01 | 0.10 | 0.10 | 0.29 |
| **8-12** | 0.00 | 0.00 | 0.00 | 0.01 | 0.01 | 0.00 | 0.09 | 0.07 | 0.18 |
| **12-16** | 0.00 | 0.00 | 0.00 | 0.00 | 0.01 | 0.00 | 0.10 | 0.03 | 0.14 |
| **16-20** | 0.00 | 0.00 | 0.00 | 0.00 | 0.01 | 0.00 | 0.07 | 0.01 | 0.09 |
| **>26** | 0.00 | 0.00 | 0.00 | 0.00 | 0.00 | 0.00 | 0.03 | 0.00 | 0.03 |
| **Grand Total** | 0.01 | 0.03 | 0.01 | 0.07 | 0.12 | 0.05 | 0.43 | 0.27 | 1.00 |

A simple linear turbulence model (Mason-sykes model, Musselman et al. 2015) was applied to a digital elevation model (DEM) of the Saddle to produce wind speed tables for primary wind directions: north, northeast, east, southeast, south, southwest, west, and northwest. Wind direction data (**Table 1)** was used to weight wind tables accordingly and produce an averaged wind speed table of the Saddle, which was used for further analysis (*Figure 4*). Values from the weighted table were used for linear regression modeling.

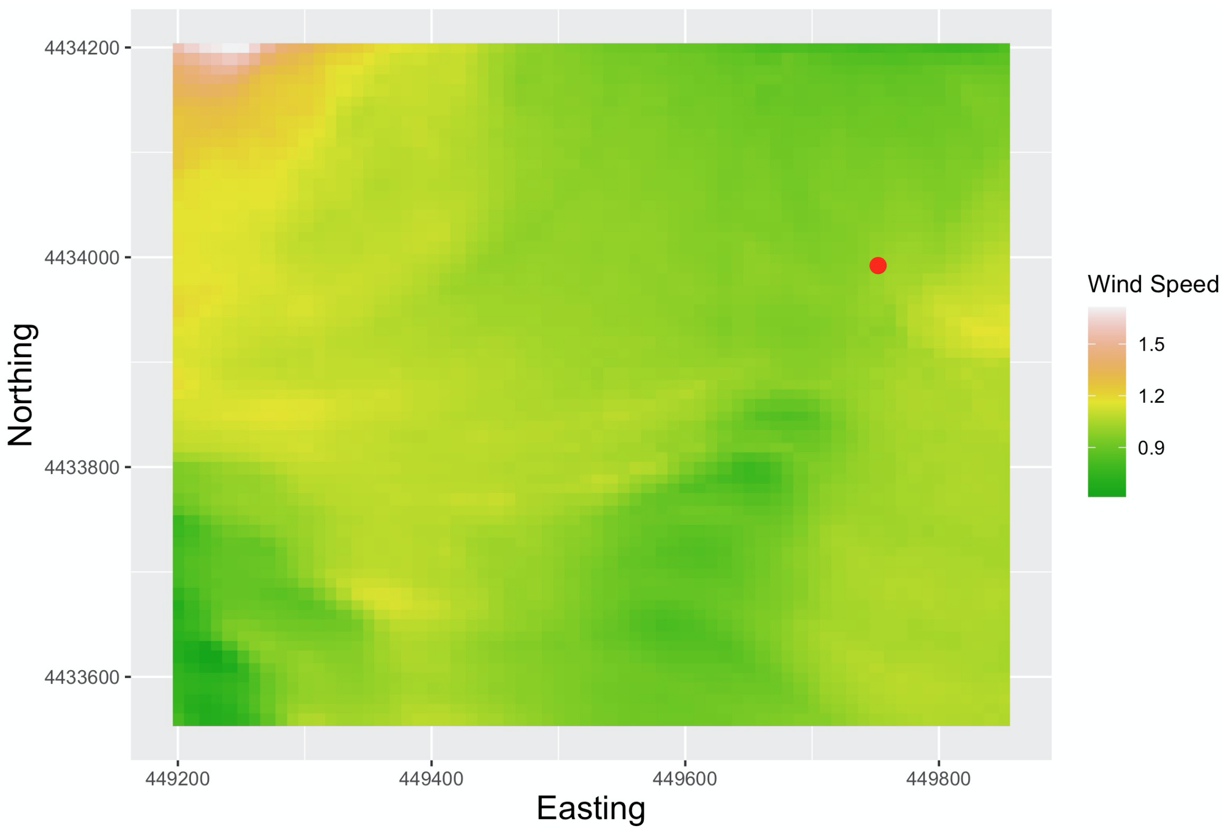


*Figure 4.* Wind distribution over the saddle catchment relative to the Saddle Meteorological station, indicated by a red point. Wind speed tables from primary wind directions were weighted to produce a comprehensive windflow map.

*Light Detection and Ranging (LiDAR)*

Light Detection and Ranging (LiDAR) is an active remote sensing method commonly used to detect snow depth across rugged, variable terrain (Deems et al., 2013). For this study, LiDAR acquisition was conducted using airborne LiDAR mounted upon a UAV (unmanned aerial vehicle) with an accompanying GPS. An IMU determined the orientation (roll, pitch, and yaw) of the airborne sensor. The return time of a transmitted laser pulse was used to calculate the location of the signal (Deems et al., 2013). Snow depth is calculated by differencing snow-free and snow-covered datasets (Deems et al., 2013).

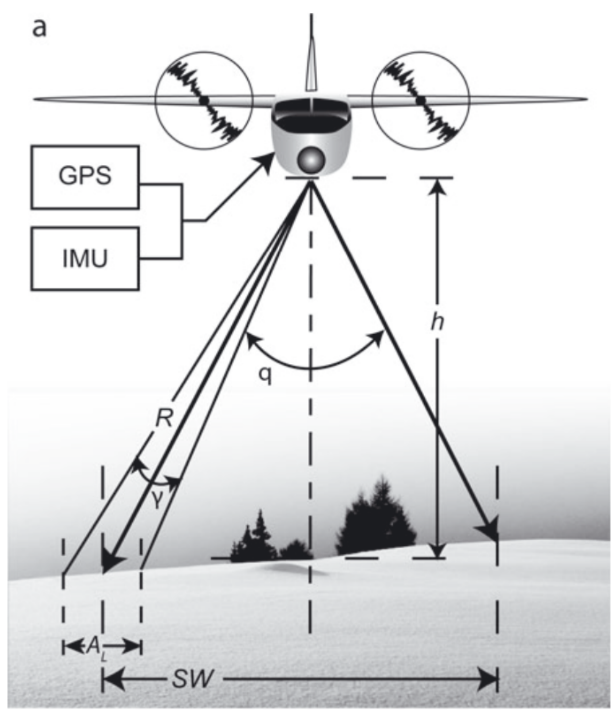


*Figure 5.* Deems et al., 2013. Depiction of the geometry of an airborne LiDAR scanner, where *R* represents range measurement, *h* the height of the scanner, and *SW* the swath width. The GPS and IMU are positioned on the UAV.

*Ground Penetrating Radar*

The two-way travel time (TWT) of 800 and 1600 MHz GPR waves was used to measure the permittivity of snow and calculate the snowpack density and LWC while LiDAR data was used to determine snow depth (Webb et al. 2018). While the GPR pulse reflects changes in snow density and LWC, the strongest signal comes from the SSI (Webb et al. 2018). The velocity of GPR waves can be determined through the following calculation:

$$v = \frac{d_s}{(TWT/2)}$$

Where $d_s$ is the depth of snow and $v$ is the velocity of GPR waves (Webb et al. 2018 (b)). The velocity of GPR waves is then used to calculate snowpack permittivity:

$$\varepsilon_{eff} = (\frac{v}{c})^2$$

Where $\varepsilon_{eff}$ is the permittivity of snow and $c$ is the speed of light in a vacuum (Webb et al. 2018). Permittivity is affected by LWC in snow and can therefore be used to approximate snowpack volumetric LWC. Final bulk volumetric LWC is calculated by the 3-way mixing model:

$$\theta w = \frac{{\varepsilon_{eff}}^{.05} - \frac{\rho d}{\rho i}\, \varepsilon_w^{0.05} - (1 - \frac{\rho d}{\rho i})\varepsilon_a^{0.05}}{\varepsilon_w^{0.05} - \varepsilon_a^{0.05}}$$

Where $\theta w$ is bulk LWC, $\rho d$ is the density of dry snow, $\rho i$ is the density of ice, $\varepsilon_w$ is the permittivity of water, and $\varepsilon_a$ is the permittivity of air. The density of snow was measured at two snow pits at the study site, and density was averaged between them. Calculated LWC volumes were capped at 0.3 as values greater than this were deemed improbable and therefore indicative of error.

*Figure 6.* Images of the drone-based airborne LiDAR (a) and GPR (b).

The GPR was towed in a sled along regular transects across the saddle, with indiscernible disruption to the snow by the sled and those pulling the GPR. A GPS attached to the sled upon which the GPR was pulled recorded the precise location of GPR measurements, allowing the GPR data to be compared to LiDAR data at precise locations. GPR GPS coordinates were used as extraction points for slope, aspect, and elevation rasters.

GPR surveys were conducted weekly over the course of the melt season: the beginning of May through melt out in July. LiDAR surveys were conducted bi-monthly. To account for the discrepancies in LiDAR and GPR temporal resolution, data from LTER snow depth sensors supplemented snow depth measurements. An example of GPR transects overlaid on LiDAR snow depth data can be seen in *Figure 7.*

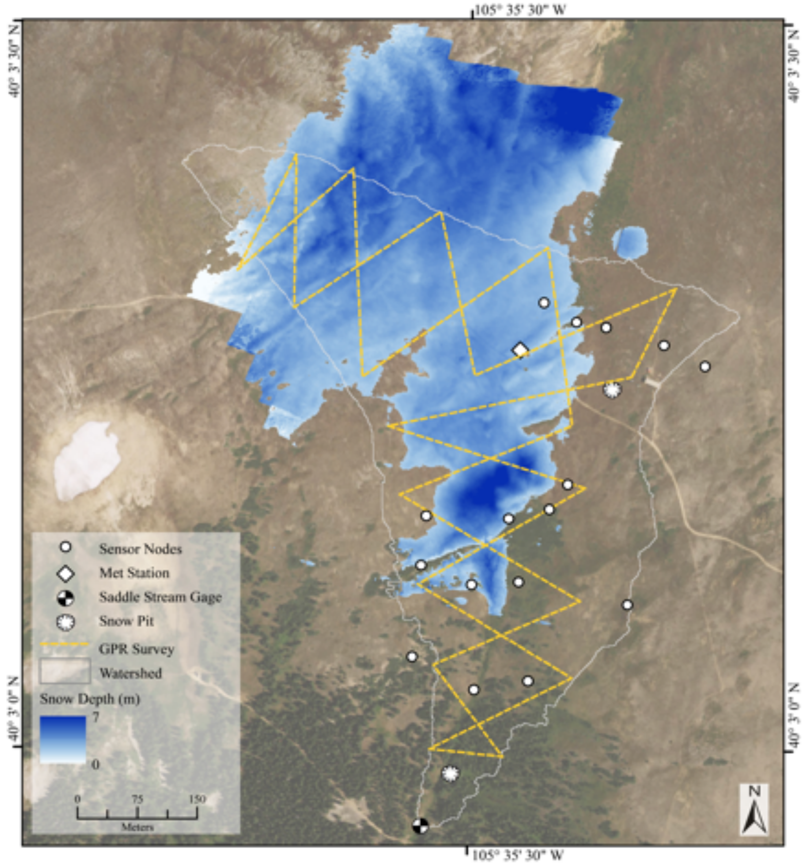


*Figure 7.* Proposed GPR survey overlaid on example snowpack on the Saddle catchment. Image courtesy of Leanne Lestak.

*Slope and Aspect Mapping*

Slope and aspect data was extracted from a resampled 10-meter bare earth DEM of the Saddle Catchment (*Figure 2)*. The DEM and slope and aspect rasters were resampled to 3-meter resolution to be consistent with snow depth map spatial resolution. Slope angle ranged from 1°-27°. Of the coordinates evaluated, 75% were southeast facing, 10% were east facing, 14% were south facing, and less than 1% were southwest facing.

*Linear Regression and Alternative Regression Modeling*

Simple linear regression modeling was used to evaluate the relationship between volumetric LWC and snow depth, aspect, slope, and elevation and the relationship between snow depth and windflow. GPS locations from the GPR were used to extract data at precise locations from windflow, elevation, aspect, slope, and snow depth rasters. Time series of $R^2$values across survey dates were observed to determine how relationships between variables changed over the course of the melt season. Significance of relationships was evaluated as a significance level of 0.05.

## Results

*Simple Linear Regression*

The correlation coefficients and $R^2$values of simple linear regression modeling are displayed in **Table 2** and **Table 3**, respectively**.** Snow depth and volumetric LWC displayed strong correlation while LWC by aspect, slope, and elevation displayed weaker correlation. Regressions of snow depth and wind speed are shown separately (**Table 4**), as this is primarily an accumulation rather than ablation season process. Nonetheless, at a p-value of 0.05, all relationships were significant.

**Table 2.** Correlation coefficients of linear regression models for ablation season processes by each survey date. Column titles indicate which variables are regressed, with dependent variables listed first.

| Survey Date | LWC by Depth | LWC by Slope | LWC by Aspect | LWC by Elevation |
|---|---|---|---|---|
| **17-May-20** | **-0.67** | **-0.05** | **0.36** | **-0.28** |
| **23-May-20** | **-0.68** | **-0.42** | **0.33** | **-0.30** |
| **27-May-20** | **-0.67** | **-0.45** | **0.30** | **-0.21** |
| **31-May-20** | **-0.70** | **-0.37** | **0.32** | **-0.21** |
| **7-Jun-20** | **-0.68** | **-0.49** | **-0.15** | **0.38** |

| | | | | |
|---|---|---|---|---|
| **14-Jun-20** | **-0.57** | **-0.43** | **0.26** | **-0.20** |
| **20-Jun-20** | **-0.67** | **-0.30** | **0.45** | **-0.35** |
| **26-Jun-20** | **-0.69** | **-0.39** | **0.42** | **-0.31** |
| **27-Jun-20** | **-0.68** | **-0.36** | **0.44** | **-0.35** |
| **Average** | **-0.67** | **-0.36** | **0.30** | **-0.20** |

**Table 3.** $R^2$values of linear regression models for ablation season processes by each survey date. Column titles indicate which variables are regressed, with dependent variables listed first.

| Survey Date | LWC by Depth | LWC by Slope | LWC by Aspect | LWC by Elevation |
|---|---|---|---|---|
| **17-May-20** | **0.45** | **0.00** | **0.13** | **0.08** |
| **23-May-20** | **0.46** | **0.18** | **0.11** | **0.09** |
| **27-May-20** | **0.45** | **0.20** | **0.09** | **0.05** |
| **31-May-20** | **0.50** | **0.14** | **0.10** | **0.04** |
| **7-June-20** | **0.46** | **0.24** | **0.02** | **0.15** |
| **14-June-20** | **0.33** | **0.18** | **0.07** | **0.04** |
| **20-June-20** | **0.45** | **0.09** | **0.20** | **0.12** |
| **26-June-20** | **0.47** | **0.15** | **0.17** | **0.09** |
| **27-June-20** | **0.47** | **0.13** | **0.19** | **0.12** |
| **Average** | **0.45** | **0.15** | **0.12** | **0.09** |

**Table 4.** Correlation coefficients and $R^2$ of linear regression models comparing snow depth to wind speed by each survey date. As wind affects snow deposition primarily in the accumulation rather than the ablation season, these regressions were separated from regressions evaluating ablation-season processes. While $R^2$ values are separated by survey date, survey date was not expected to impact the effect of wind speed on drifting.

| | 17-May-20 | 23-May-20 | 27-May-20 | 31-May-20 | 7-June-20 | 14-June-20 | 20-June-20 | 26-June-20 | 27-June-20 | **Average** |
|---|---|---|---|---|---|---|---|---|---|---|
| $R$ | 0.05 | 0.43 | 0.38 | 0.35 | 0.58 | 0.53 | 0.48 | 0.40 | 0.40 | **0.40** |
| $R^2$ | 0.00 | 0.18 | 0.14 | 0.12 | 0.33 | 0.28 | 0.23 | 0.16 | 0.16 | **0.16** |

*Linear Regression Time Series*

$R^2$ values were compared over time to observe shifts in variable control over the melt season (*Figure 8*). The relationships between $R^2$ values and survey dates were tested for significance. At a p-value of 0.05, no time series displayed a significant relationship between independent variable control and survey date. Notably, models that regressed LWC by snow depth displayed consistent $R^2$ values across survey dates.

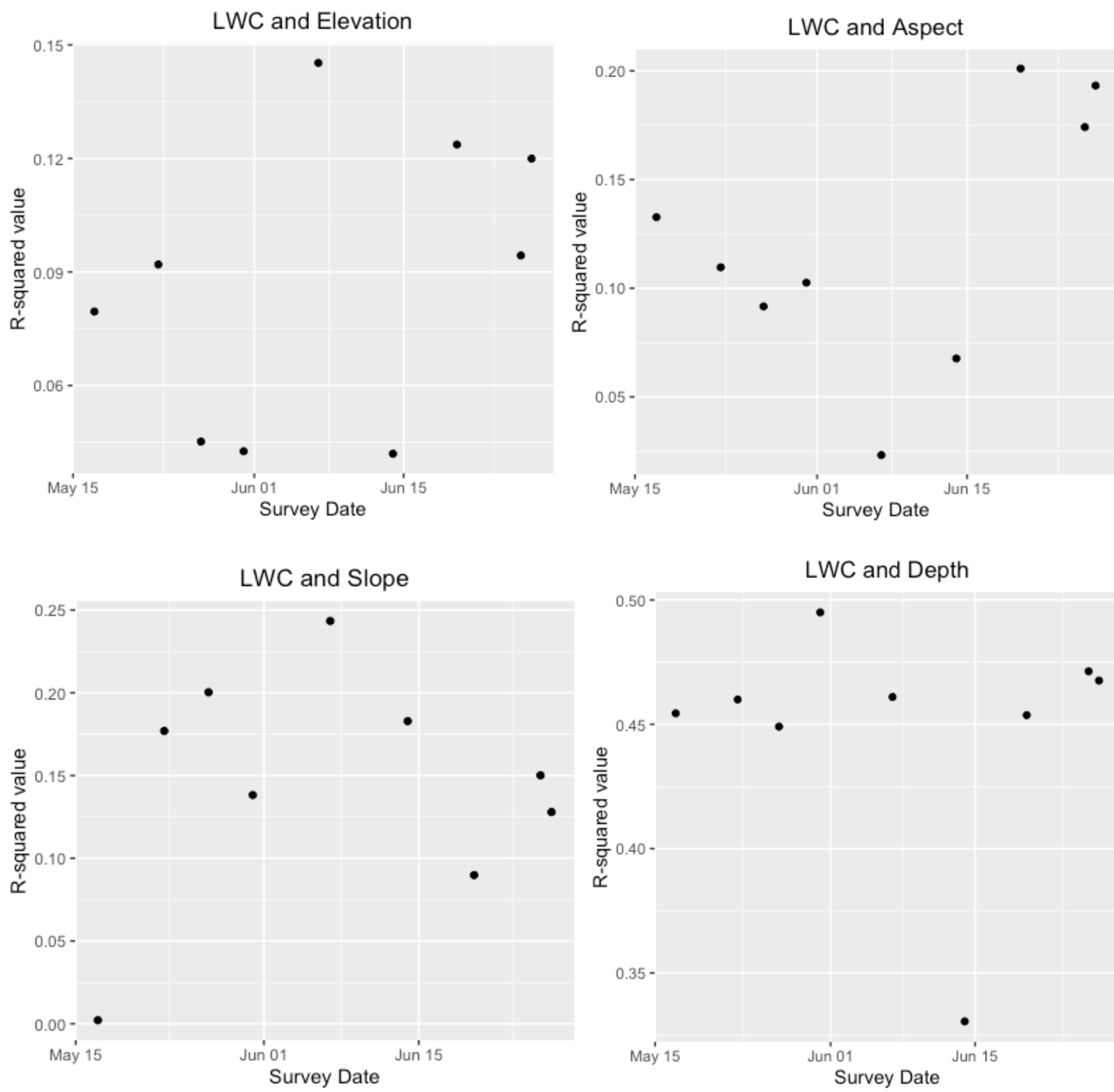


*Figure 8*. Linear regression models of $R^2$values across survey dates. A time series of wind velocity and depth was not compared across survey dates as this is an accumulation rather than a melt season process. No regressions between $R^2$ and survey date produced significant results.

*Alternative Regression Modeling*

Alternative regression models were explored for LWC versus snow depth and LWC versus slope as snow depth and slope exerted the greatest control over LWC variability (**Table 2, Table 3**). 3rd degree polynomial models produced the highest $R^2$for LWC by both snow depth and slope (*Figure 9 and 10*). A 3rd degree polynomial model that regressed LWC by snow depth:

$$y = 0.0039x^3 + 0.0409x^2 - 0.1503x + 0.3$$

produced an $R^2$ value of 0.5899. A 3rd degree polynomial model that regressed LWC by slope:

$$y = 0.0001x^3 + 0.0061x^2 - 0.0789x + 0.4496$$

produced an $R^2$ value of 0.2641.

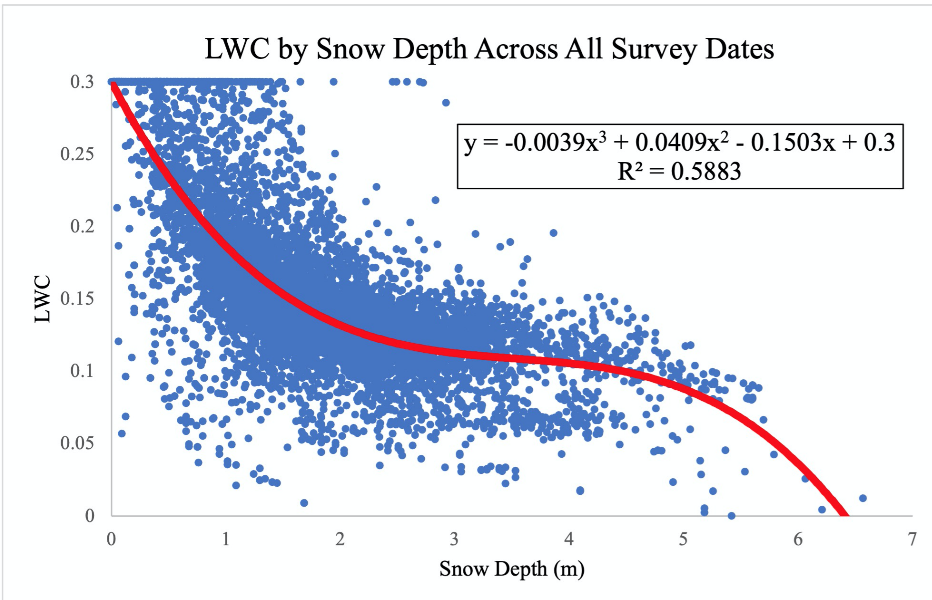


*Figure 9.* A 3rd degree polynomial model best explains the relationship between LWC and snow depth. The $R^2$ value of this model is 0.5899.

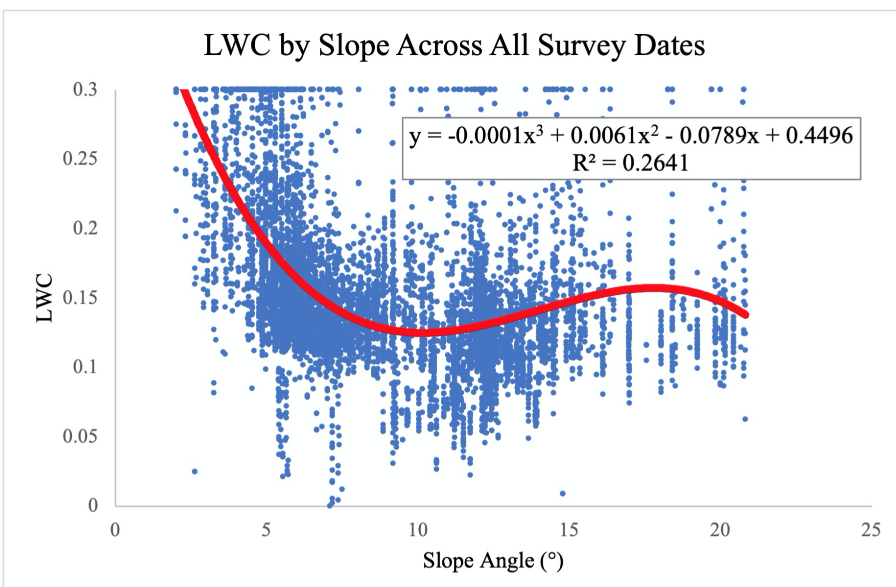


*Figure 10.* A 3rd degree polynomial model best explains the relationship between LWC and slope. The $R^2$ value of this model is 0.2641.

## Discussion

The results of this study indicate that snow depth exerts the greatest control on volumetric LWC. Regressions between snow depth and LWC produced an average correlation coefficient of -0.67 and an average $R^2$ value of 0.45. Aspect, slope, and elevation displayed weaker, though significant, correlations with snow LWC.

As this study was executed at the catchment scale, as opposed to the watershed or regional scale, it is possible that slope, elevation, and aspect did not exert significant control on LWC due to lack of variability at this spatial extent. In particular, the lack of variability in aspect at the Saddle hindered analysis of the relationship between LWC and aspect. Given that south facing aspects in the Northern Hemisphere experience greater radiative forcing than northern aspects, it is reasonable to expect that southern facing aspects will exhibit greater liquid water content than north, west, and east facing aspects. As all aspects at this catchment were south, east, or southeast facing, the relationship between aspect and LWC may not have been apparent despite the influence of aspect on radiative forcing and melting. Therefore, a catchment with greater aspect variability would be more suitable for determining the relationship between aspect and LWC.

A study area with greater elevation variability would similarly provide more insight into the relationship between LWC and elevation. An adequate study site for observing the impact of elevation on LWC would likely need to be at the basin or watershed scale. When transitioning from subalpine to alpine zones in the Colorado Rockies, tall vegetation disappears, enabling turbulent heat fluxes, radiation, and windflow to exert the greatest control over snowpack variability (Webb et al. 2020; Musselman et al. 2015). High elevations experience higher frequency snow events of greater magnitude compared to lower elevations, resulting in more snow and complex stratigraphy (Webb et al. 2020). Snow depth and stratigraphy impact LWC and the formation of preferential flow paths. While the impact of elevation on snow could likely be observed across climate zones where vegetation and snow events vary, elevation may not vary enough across the catchment scale to impact snow LWC.

The results of windflow and snow depth regression produced results contradictory to expected results. Typically, areas of high wind speed experience scouring while areas of low wind speed experience snow deposition and drifting (DeWalle and Rango, 2008). This relationship would lead to negative correlation between snow depth and wind speed. The results of this study, however, indicate that wind speed and snow depth are positively correlated (**Table 4**). This result, which is counter to known truths about the relationship between wind drifting and snow, is likely due to the lack of variability at the saddle, which experiences consistent winds (recall *Figure 4*, pg. 16). *Figure 4* suggests that if wind speeds at the saddle meteorological station equal 1, most other points on the saddle are only slightly above or below 1 (*Figure 11*).

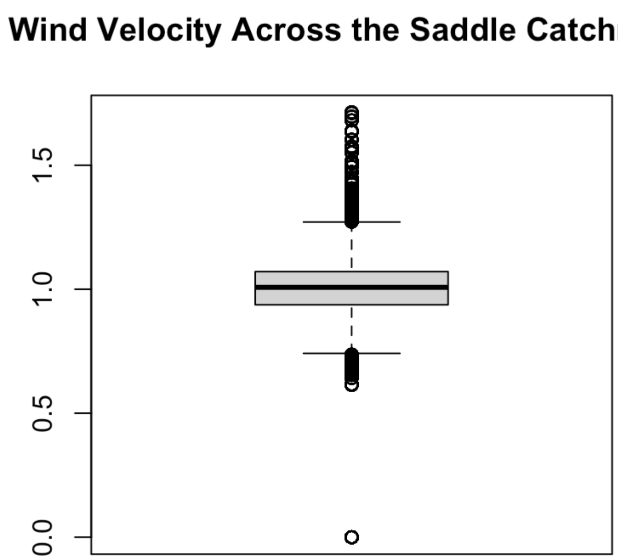


*Figure 11.* Average wind velocity relative to the Saddle Meteorological station across the Saddle Catchment. Measurements are relative to the meteorological station and are therefore unitless.

While the Saddle exhibits some variability in windflow, the variability is likely not great enough to display the threshold response that results in wind drifting and scouring. Therefore, similar to aspect and elevation data, a larger study site such as a basin or watershed scale site would be more adequate for evaluating the statistical relationship between wind speed and snow depth.

LWC and snow depth display the strongest relationship of the variables regressed. Interestingly, this relationship is negative. This finding supports the hypothesis that areas of deeper snow exhibit less volumetric LWC due to greater cold content and greater distance between preferential flow paths. Conversely, shallow snow may have greater LWC due to convergent preferential flow paths and earlier cold content satisfaction. It is important to note that while volumetric LWC is greater in shallower snow, total LWC is still greater in deeper snow (*Figure 12*). While the total quantity of LWC is greater in deeper snowpack, shallower snow has relatively greater LWC.

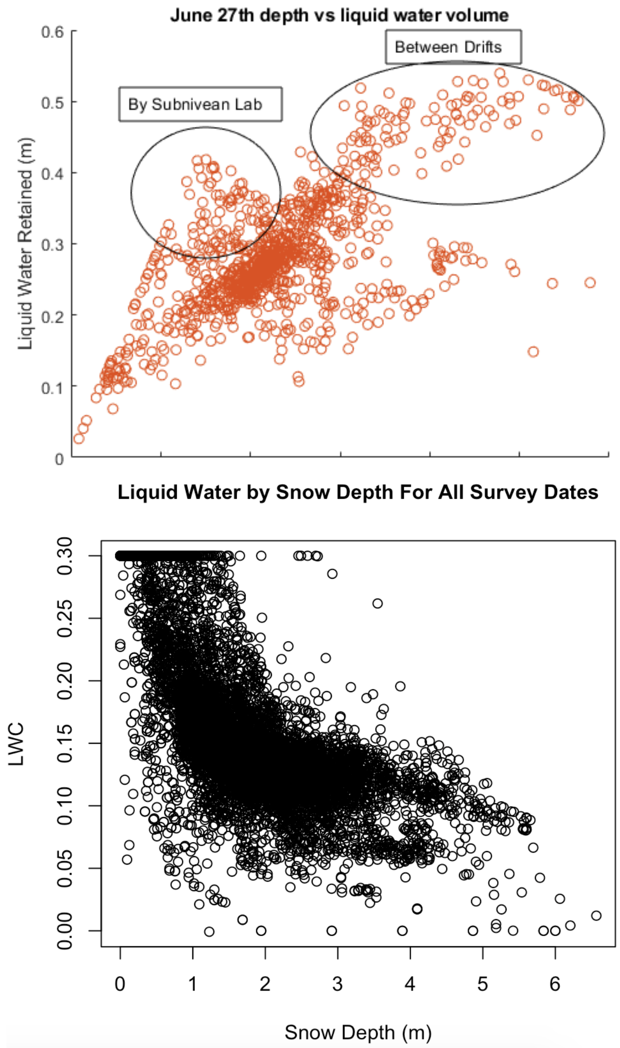


*Figure 12*. (a) Courtesy Ryan Webb (personal communication, 2021). The relationship between snow depth and total liquid water is positive. (b) The relationship between snow depth and *volumetric* liquid water is negative. Snow depth increase corresponds with greater total liquid water content while the proportional liquid water content decreases.

Both alternative regression models comparing LWC to slope and snow depth (*Figure 9* and *Figure 10*) produced higher $R^2$values than linear regression fits, suggesting that these relationships exhibit greater complexity than linear modeling can account for. While exploring why alternative regression fits trump linear regression fits for these variables is beyond the scope of this study, it is interesting to note that both regression fits exhibited asymptotic behavior between LWC values of 0.05 and 0.1. This behavior suggests that during the ablation season, across slope angle and across snow depth values, LWC of at least 0.05 may be expected.

Interestingly, linear regression models that regressed LWC by slope for each survey (*Figure 14*) displayed threshold responses characterized by the *Colbeck* [1982] classification scheme (*Figure 13*). This classification scheme identifies two stages of water saturation within snow: the pendular regime and the funicular regime (Kinar and Pomeroy 2015). The pendular regime occurs when air has a continuous path through pore space surrounding snow particles, while the funicular regime occurs when water is continuous throughout the pore space of a snowpack and air is only found as bubbles (Kinar and Pomeroy 2015). The LWC of the pendular regime ranges from < 7-14% saturation, transition zone between the pendular and funicular regimes ranges from 11-15% saturation, and the funicular regime ranges form 14-25% saturation.

LWC by slope regression models show asymptotic behavior between roughly 7-12% LWC, saturation values that are characteristic of the pendular regime. At slightly less than 15% LWC, the slope of points increases abruptly, displaying what could be interpreted as a threshold response. This pattern is particularly apparent in May 23, May 27, May 31, and June 7 regressions (*Figure 13*). This threshold response occurs at slope angle values around 0-7°, suggesting that lower angle slopes may be more likely to transition from the pendular to funicular regime.

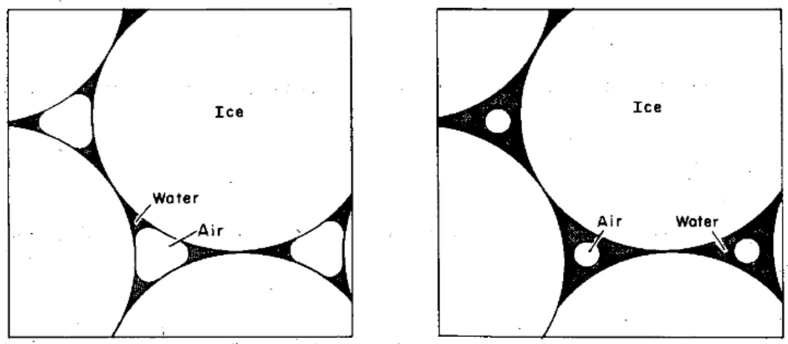


*Figure 13.* (Colbeck 1973) (a) the Pendular regime and (b) the Funicular regime. Water content of snow in the pendular regime ranges from 7-14% saturation while water content of snow in the funicular regime ranges from 14-25% saturation.

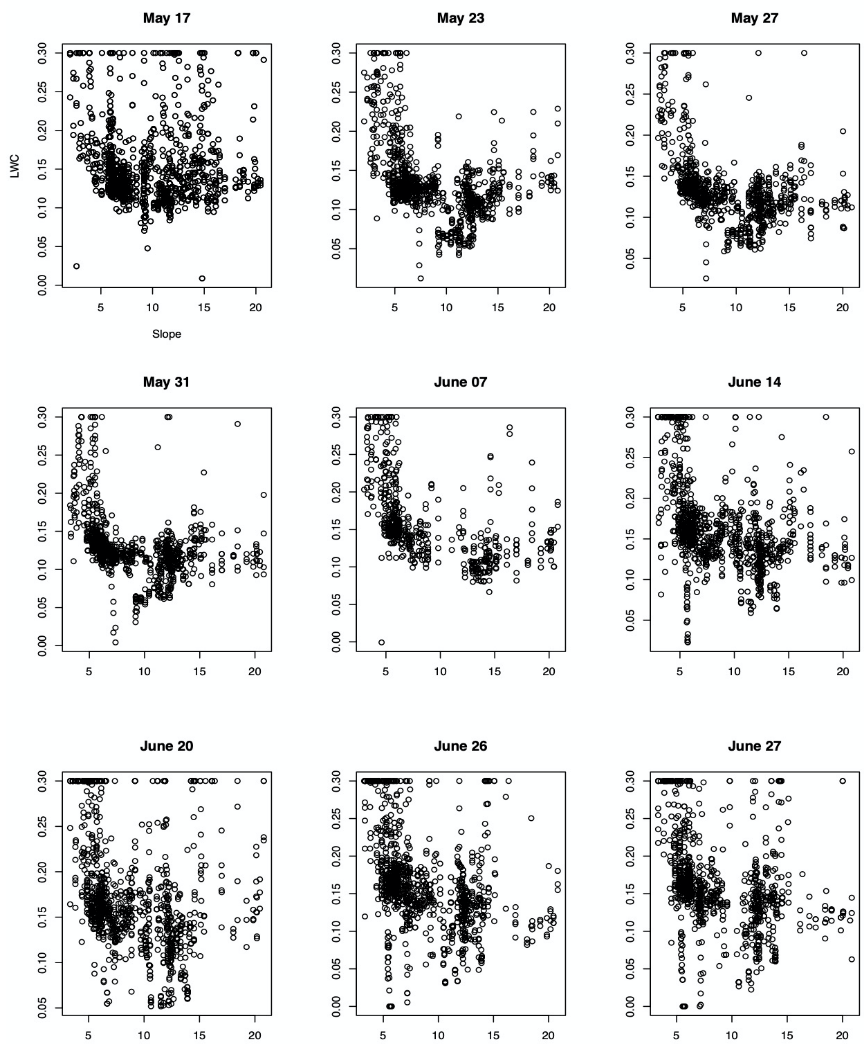


*Figure 14*. Simple linear regression models comparing LWC to slope by date, with survey date indicated at the top of each regression plot. Threshold response can be seen at the transition between the pendular and funicular regimes at 11-15% LWC, particularly for survey dates May 23, May 27, May 31, and June 07.

This threshold behavior at the interface of the pendular and funicular regimes can also be seen in models regressing LWC by depth (*Figure 12* (b); Appendix, *Figure 14*). This trend can be observed in regressions of LWC by depth for both daily and seasonal linear regression models.

## Conclusions and Future Work

Linear regression modeling suggests that snow depth exerts the greatest control on volumetric LWC in the Saddle snowpack while slope, aspect, and elevation explain less of the variability in LWC. Areas of deep snow displayed the smallest volumetric LWC, likely due to the greater cold content and greater distance between preferential flow paths of deeper snow columns as compared to shallower snow. Snow depth presents a single reliable variable for predicting LWC in snow.

While nearly all p-values of independent and dependent variables indicated significant results, $R^2$values were generally low for independent variables besides snow depth. A study site with greater aspect and elevation variability would likely provide greater insight into the control these variables exert on LCW. As slope, aspect, elevation, and snow depth all exert some amount of control on volumetric LWC, multiple regression modeling may produce higher $R^2$values.

The non-linear relationship between LWC and snow depth and LWC and slope offer grounds for future work. The complexity of these relationships is beyond what can be explained through simple linear regression. The asymptotic behavior of these regressions suggests:

a. Regardless of snow depth or slope, liquid water is present in all points of a melting snowpack.

b. As this behavior occurs at the interface of the pendular and funicular regimes, this may be indicative of a threshold response when LWC in a snowpack surpasses the pendular regime, though greater investigation is needed to validate this observation.
c. Slope angles ranging 0° - ~7° may be most likely to hold liquid water and transition from the pendular to funicular regimes.

Given that saturation levels characterized by the funicular regime greatly increase snowpack permeability as capillary pressure is reduced (Colbeck 1973), a threshold response when transitioning from pendular to funicular levels of saturation would make sense, though additional work would be required to confirm this observation.

## Acknowledgments

I would like to give so much thanks to my lab group, INSTAAR's Mountain Hydrology Group. The guidance and inspiration from this group has shaped my professional aspirations in ways I couldn't have imagined prior to joining them as a field assistant. Particularly in light of the Covid-19 pandemic, the Mountain Hydrology lab group transformed my undergraduate career.

I'd like to thank my advisors, Dr. Keith Musselman and Dr. Noah Molotch. Dr. Musselman guided me every step of the way, and I am hugely grateful for his availability and clear dedication to mentoring me through my project. He has modeled for me how to use snow science as a method for pursuing social equity, and I hope to instill similar ethics in my own research down the line. Dr. Noah Molotch has offered invaluable guidance and leadership, and I am grateful for his commitment to the academic and professional development of his students. I have felt exceedingly well cared for while advised by Dr. Molotch, and I am deeply appreciative of the community that he's crafted through the Mountain Hydrology Group. I am grateful for Dr. Ryan Webb's support throughout this project. It has been exciting and enriching to learn from his expertise on liquid water in snow.

I would also like to thank my great friend and mentor, Kate Hale. Kate has provided me with tremendous support personally and professionally, and I am excited to continue working with her as a part of the snow science community. I am very grateful to all other members of my lab group. In particular, Kehan Yang and Leanne Lestak both supported my project through lending their skills in coding and GIS, respectively, which I deeply appreciate and which greatly advanced my project.

I would also like to acknowledge that my university, the University of Colorado at Boulder, sits upon land within the territories of the Ute, Cheyenne, and Arapaho peoples and that 48 contemporary tribal nations are historically tied to the lands that make up the state of Colorado.

## Works Cited


Barnett, T. P., J. C. Adam, and D. P. Lettenmaier. 2005. “Potential Impacts of a Warming Climate on Water Availability in Snow-Dominated Regions.” *Nature* 438 (7066): 303–9.

Barnhart, Theodore B., Noah P. Molotch, Ben Livneh, Adrian A. Harpold, John F. Knowles, and Dominik Schneider. 2016. “Snowmelt Rate Dictates Streamflow: Snowmelt Rate Dictates Streamflow.” *Geophysical Research Letters* 43 (15): 8006–16.

Colbec, Samuel C. n.d. “Theory of Metamorphism of Wet Snow.” Accessed March 30, 2021. https://erdc-library.erdc.dren.mil/jspui/bitstream/11681/5894/1/CRREL-Research-Report-313.pdf.

DeWalle, David R., and Albert Rango. 2008. *Principles of Snow Hydrology*. Cambridge University Press.

Eiriksson, David, Michael Whitson, Charles H. Luce, Hans Peter Marshall, John Bradford, Shawn G. Benner, Thomas Black, Hank Hetrick, and James P. McNamara. 2013. “An Evaluation of the Hydrologic Relevance of Lateral Flow in Snow at Hillslope and Catchment Scales: LATERAL FLOW IN SNOW.” *Hydrological Processes* 27 (5): 640–54.

Harpold, Adrian A., Noah P. Molotch, Keith N. Musselman, Roger C. Bales, Peter B. Kirchner, Marcy Litvak, and Paul D. Brooks. 2015. “Soil Moisture Response to Snowmelt Timing in Mixed-Conifer Subalpine Forests: SOIL MOISTURE RESPONSE TO SNOWMELT.” *Hydrological Processes* 29 (12): 2782–98.

Heilig, A., C. Mitterer, L. Schmid, N. Wever, J. Schweizer, H.P. Marshall, and O. Eisen. 2015. “Seasonal and Diurnal Cycles of Liquid Water in snow—Measurements and Modeling.” *Journal of Geophysical Research. Earth Surface* 120 (10): 2139–54.

Jeffrey S.Deems, Thomas H. Painter, David C.Finnegan. n.d. “Lidar Measurement of Snow Depth: A Review.” Accessed March 21, 2021. https://doi.org/10.3189/2013JoG12J154.

Kinar, N. J., and J. W. Pomeroy. 2015. “Measurement of the Physical Properties of the Snowpack: MEASUREMENT OF SNOWPACK.” *Reviews of Geophysics* 53 (2): 481–544.

Li, Dongyue, Melissa L. Wrzesien, Michael Durand, Jennifer Adam, and Dennis P. Lettenmaier. 2017. “How Much Runoff Originates as Snow in the Western United States, and How Will That Change in the Future?: Western U.S. Snowmelt-Derived Runoff.” *Geophysical Research Letters* 44 (12): 6163–72.

López-Moreno, J. I., S. R. Fassnacht, S. Beguería, and J. B. P. Latron. 2011. “Variability of Snow Depth at the Plot Scale: Implications for Mean Depth Estimation and Sampling Strategies.” *The Cryosphere* 5 (3): 617–29.

Mitterer, Christoph, Achim Heilig, Jürg Schweizer, and Olaf Eisen. 2011. “Upward-Looking Ground-Penetrating Radar for Measuring Wet-Snow Properties.” *Cold Regions Science and Technology* 69 (2): 129–38.

Molotch, Noah P., and Roger C. Bales. 2006. “Comparison of Ground-Based and Airborne Snow Surface Albedo Parameterizations in an Alpine Watershed: Impact on Snowpack Mass Balance: COMPARISON OF SNOW ALBEDO PARAMETERIZATIONS.” *Water Resources Research* 42 (5). https://doi.org/10.1029/2005wr004522.

Musselman, Keith N., Martyn P. Clark, Changhai Liu, Kyoko Ikeda, and Roy Rasmussen. 2017. “Slower Snowmelt in a Warmer World.” https://doi.org/10.1038/nclimate3225.

Musselman, Keith N., Flavio Lehner, Kyoko Ikeda, Martyn P. Clark, and Roy Rasmussen. 2018. “Projected Increases and Shifts in Rain-on-Snow Flood Risk over Western North America” 8 (9)). https://doi.org/10.1038/s41558-018-0236-4.

Musselman, Keith N., John W. Pomeroy, Richard L. H. Essery, and Nicolas Leroux. 2015. “Impact of Windflow Calculations on Simulations of Alpine Snow Accumulation, Redistribution and Ablation: Windflow Models Impact Simulations of Alpine Blowing Snow and Melt.” *Hydrological Processes* 29 (18): 3983–99.

Rauscher, Sara A., Jeremy S. Pal, Noah S. Diffenbaugh, and Michael M. Benedetti. 2008. “Future Changes in Snowmelt-Driven Runoff Timing over the Western US.” *Geophysical Research Letters* 35 (16). https://doi.org/10.1029/2008gl034424.

Trujillo, Ernesto, Noah P. Molotch, Michael L. Goulden, Anne E. Kelly, and Roger C. Bales. 2012. “Elevation-Dependent Influence of Snow Accumulation on Forest Greening.” *Nature Geoscience* 5 (10): 705–9.

Webb, R. W., K. S. Jennings, M. Fend, and N. P. Molotch. 2018. “Combining Ground-Penetrating Radar With Terrestrial LiDAR Scanning to Estimate the Spatial Distribution of Liquid Water Content in Seasonal Snowpacks.” *Water Resources Research* 54 (12): 640.

Webb, R. W., M. W. Williams, and T. A. Erickson. 2018. “The Spatial and Temporal Variability of Meltwater Flow Paths: Insights From a Grid of Over 100 Snow Lysimeters.” *Water Resources Research* 54 (2): 1146–60.

Webb, Ryan W. 2017. “Using Ground Penetrating Radar to Assess the Variability of Snow Water Equivalent and Melt in a Mixed Canopy Forest, Northern Colorado.” *Frontiers of Earth Science* 11 (3): 482–95.

Webb, Ryan W., Fassnacht, Steven R., Gooseff, Michael N. 2017.“Defining the Diurnal Pattern of Snowmelt Using a Beta Distribution Function.” *Journal of the American Water Resources Association* 53 (3): 684–96.

Webb, Ryan W., Fassnacht, Steven R., Gooseff, Michael N. 2018. “Hydrologic Flow Path Development Varies by Aspect during Spring Snowmelt in Complex Subalpine Terrain.” *The Cryosphere* 12 (1): 287–300.

Webb, Ryan W., Oliver Wigmore, Keith Jennings, Mike Fend, and Noah P. Molotch. 2020. “Hydrologic Connectivity at the Hillslope Scale through Intra-snowpack Flow Paths during Snowmelt.” *Hydrological Processes* 34 (7): 1616–29.

Westerling, A. L., H. G. Hidalgo, D. R. Cayan, and T. W. Swetnam. 2006. “Warming and Earlier Spring Increase Western U.S. Forest Wildfire Activity.” *Science* 313 (5789): 940–43.

Winchell, Taylor S., David M. Barnard, Russell K. Monson, Sean P. Burns, and Noah P. Molotch. 2016. “Earlier Snowmelt Reduces Atmospheric Carbon Uptake in Midlatitude Subalpine Forests: EARLIER SNOWMELT REDUCES CARBON UPTAKE.” *Geophysical Research Letters* 43 (15): 8160–68.

## Appendix

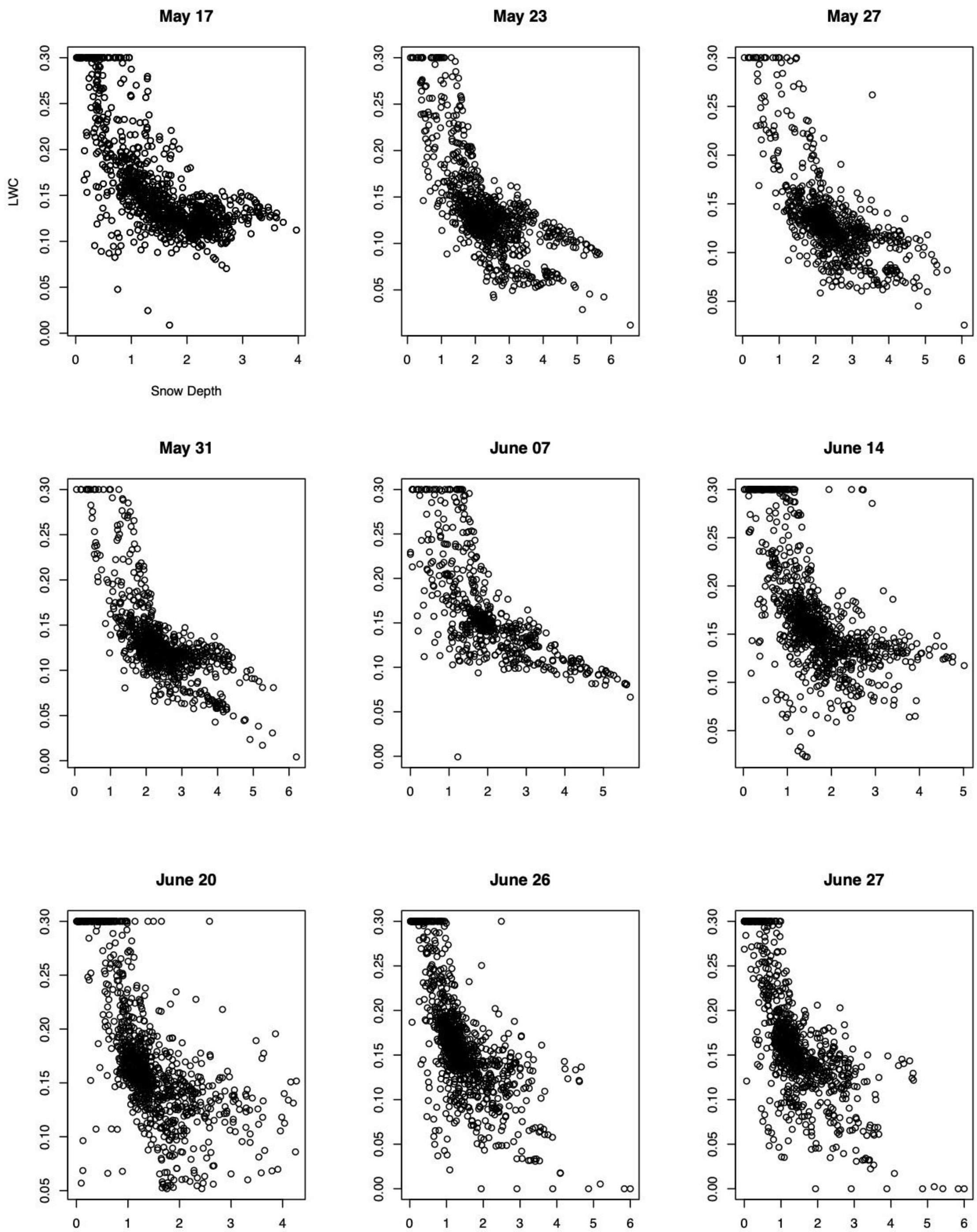


*Figure 15*. Simple linear regression models comparing LWC to snow depth by survey date, indicated at the top of each regression plot.

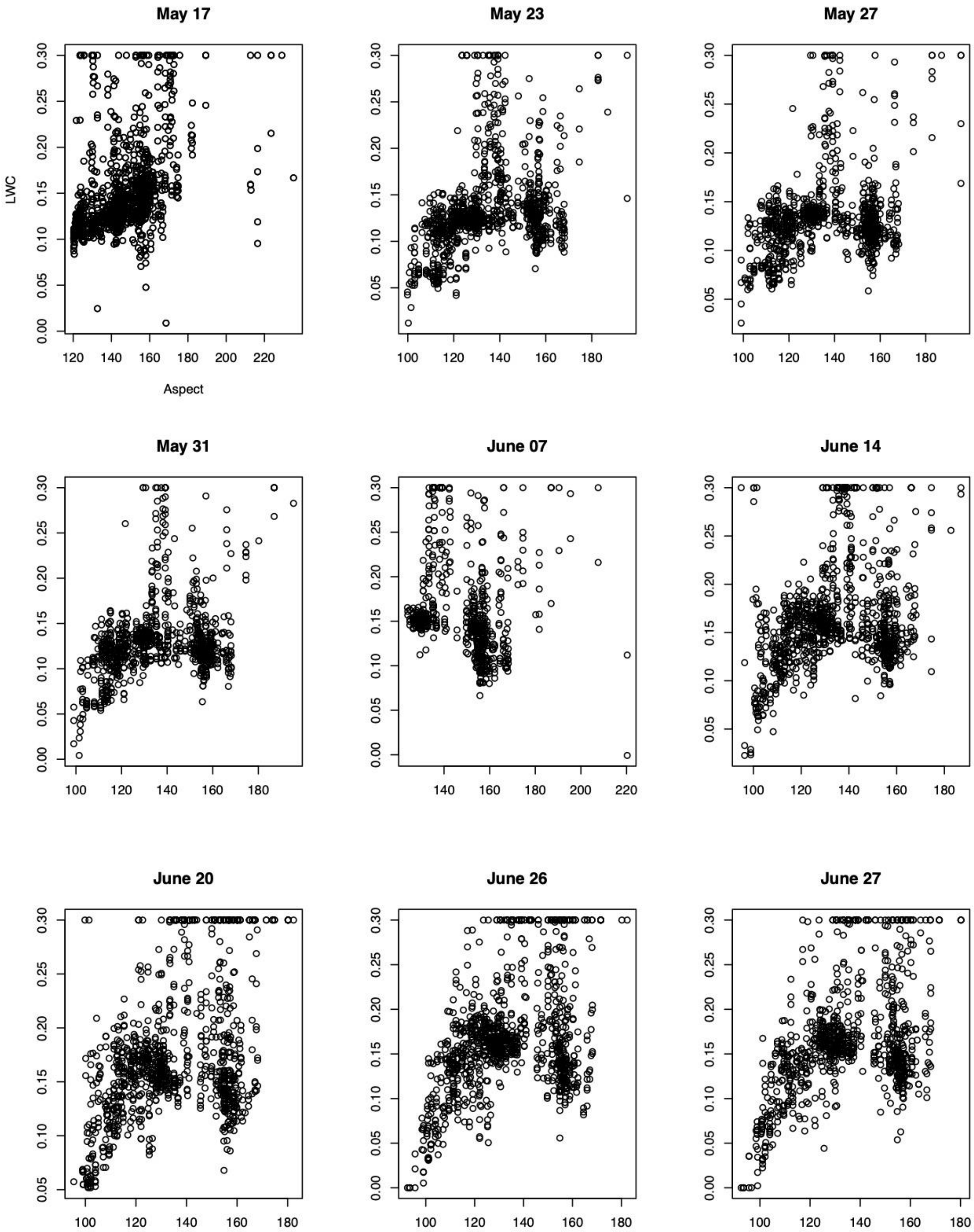


*Figure 16*. Simple linear regression models comparing LWC to aspect by survey date, indicated at the top of each regression plot.

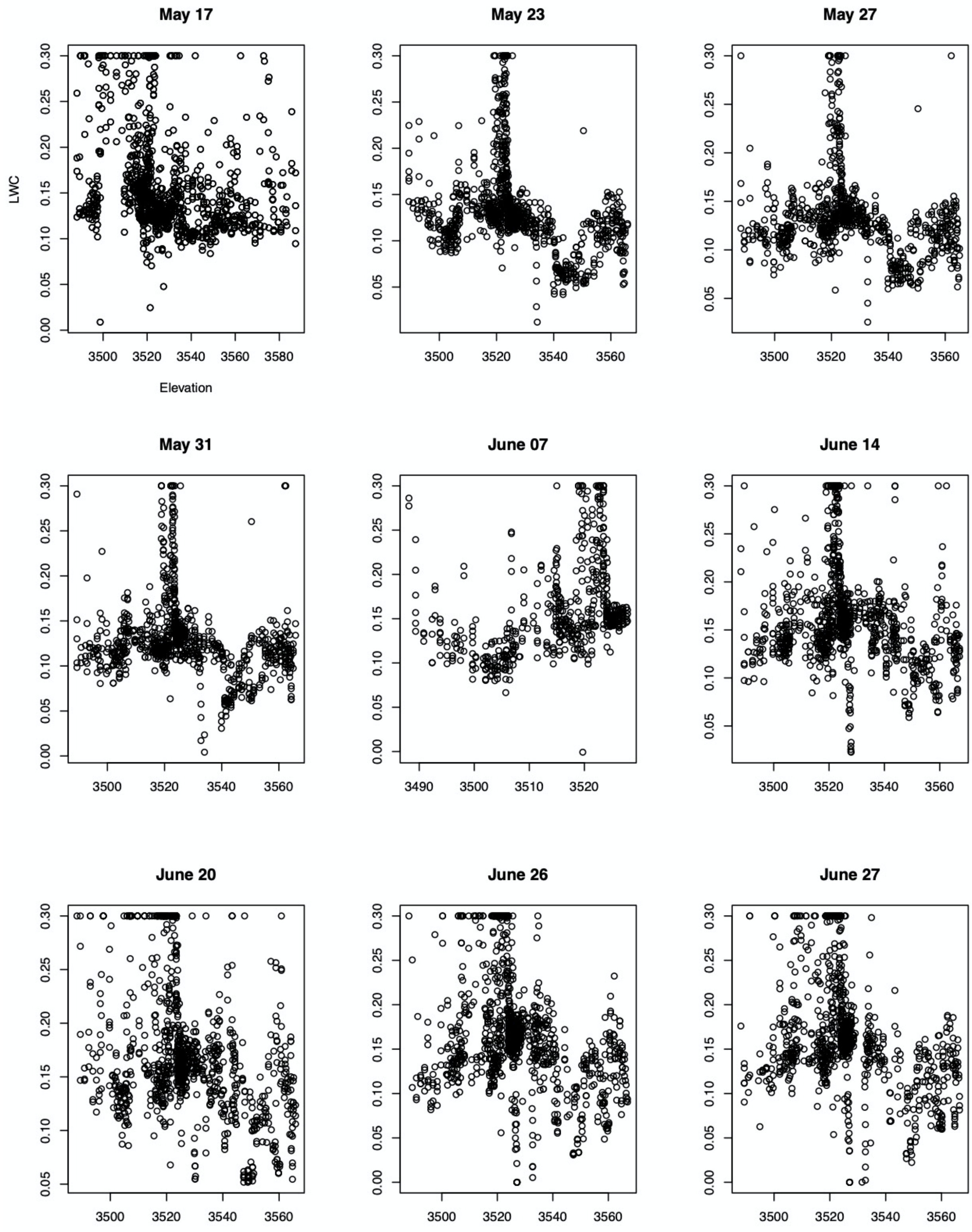


*Figure 17*. Simple linear regression models comparing LWC to elevation by survey date, indicated at the top of each regression plot.